CHAPTER 4

Crustal Gravity and Magnetic Anomaly Correlations of Greenland

(JGR or Geophysics: 20-25 pages text)

Abstract

To increase understanding of the regional geology and structure for the Greenland area (58.7 - 84.2° N and 285.75 - 349.50°), the distribution of correlative components between aeromagnetic (MA) and the free-air gravity (FAGA) anomalies was investigated. In particular, crustal features located in the Labrador Sea margins are examined to determine possible lithologies and their relevance to the tectonic evolution of the region. Spectral correlation theory was used to compare the first vertical derivative FAGA with reduced-to-pole MA. The more prominent positively and negatively correlated anomalies suggested generalized crustal distributions of magnetization and density for the region. Correlative FAGA and MA maxima tended to reflect the presence of gneisses in continental terrain and serpentinized mantle in offshore coastal areas, while correlative minima tended to overlie sedimentary basins, granitic terrains, and regions of crustal faulting. Shallow or exhumed unserpentized mantle and marginally magnetized continental rocks tended to be characterized by negative correlations of FAGA maxima and MA minima, while FAGA minima and

MA maxima characterized the continent-ocean boundary at the shelf break. Null correlated MA and FAGA minima or maxima characterized the boundary between the Nagssugtoqidian and Rinkian Mobile belts. Null correlated FAGA and MA minima or maxima characterized the oceanic crust parallel to the Rekjaynes Ridge, probably representing remanent magnetization. These results are combined with features of a gravity-derived Moho map and seismic survey data to identify regions of possibly extended and rifted crust off the southwestern and southeastern coasts of Greenland.

4.1 Introduction

In Chapter 3, a depth to Moho model determined for the Greenland study area (58.7 - 84.2° N and 285.75 - 349.50°) suggested the presence of deep roots subparallel to the southwestern Greenland coast that have been modeled by seismic surveys as transitional and rifted continental crust [Chian and Louden, 1994; Chian et al., 1995a; 1995b]. However, Srivastava and Roest [1995] modeled this same region using oceanic crust starting at the Greenland shelf break, because kinematic analysis of the relative positions and movement of North America and Eurasia required the continent-ocean boundary to occur there to minimize plate overlaps at closure. Analysis of potential field data for the Greenland margin may help to determine if the crust is either purely oceanic [Srivastava and Roest, 1995], continental [Chalmers and Laursen, 1995], or transitional [Chian et al., 1995a; 1995b].

To better determine the crustal properties for this and other regions in Greenland, both gravity and magnetic anomaly data for all of Greenland are correlated to define broad regions containing similar characteristics. Taken in the light of available geologic survey data, these data are used to limit the lithologies and refine crustal structures.

Previous geologic studies have mapped the margins relatively well [Escher and Pulvertaft, 1995; Okulitch, 1991], but the extension of these geologic features under the ice and offshore is poorly understood. Although these obscured regions cannot be observed directly, coverage of free-air gravity (FAGA) and magnetic (MA) anomalies has become available for this region recently to constrain subsurface density and magnetization properties that may be interpreted for new insight on the geologic evolution of Greenland and its surrounding regions.

The tectonic development of the study region resulted in the emplacement of geologic features that commonly involve correlative density and magnetization variations. However, only regional comparisons will be made due to the wide range of processes that can cause significant local variability in densities and magnetic susceptibilities [von Frese, 1981].

The non-uniqueness of geophysical solutions complicates the relationship between FAGA and source rock densities. However, while longer wavelength components of FAGA may be due to broad shallow sources or from deeper sources [Anderson, 1998], isostatic compensation on a regional basis would indicate that the shorter wavelength FAGA ($< 3^\circ$ or about 350 km wavelength) are more likely due only to lithospheric sources [von Frese, 1981].

The relationship between MA and the magnetic susceptibility is complicated by chemical and physical processes that may locally remove or modify the magnetic components within the source rocks and cause an extreme range of values [von Frese, 1981]. While an analysis of shorter wavelength components of both the FAGA and MA may offer insight into smaller scale structures, this analysis will be made on more regional features such as the extents of geologic provinces or the crustal structure along the southwestern Greenland margin.

This study focused on identifying and interpreting correlative features in the FAGA and MA derived from intracrustal sources by first isolating and then removing components in the FAGA and MA related to thickness variations, as well as sub-crustal sources for the FAGA. The intracrustal FAGA and MA were then compared by spectral correlation analysis [von Frese et al., 1997] for correlative features.

In the following sections, geologic background for the study region is reviewed and the use of spectral correlation theory for isolating correlative features in FAGA and MA is described and implemented. The geologic significance of these correlative anomalies is considered in the context of the gravity-derived Moho model [Chapter 3] shown in Figure 4.1 and available geologic information [Escher and Pulvertaft, 1995; Okulitch, 1991].

4.2 Greenland Geology and Related Density and Magnetization Variations

Mapping of Greenland's geology has been limited mostly to the relatively ice-free coastal regions [Escher and Pulvertaft, 1995; Okulitch, 1991]. These regions consist mostly of igneous rocks intruded into gneissic country rock with relatively limited sedimentary cover. These rock types can reflect a range of anomaly-producing density and magnetization variations [Turcotte and Schubert, 1982; Ahrens, 1995; Escher and Watt, 1976; Toft and Arkani-Hamed, 1993; Friend et al., 1996; Chian and Louden, 1992].

To generalize the relationships between the anomaly-producing physical property variations and the crustal geology of Greenland, this study relied on the description of rock types and features of the major provinces in Escher and Watt [1976] and Brozena [1995], as well as the synthesis of physical properties for the rocks of the U.S. midcontinent in Jones [1988]. This synthesis is appropriate due to similarities in

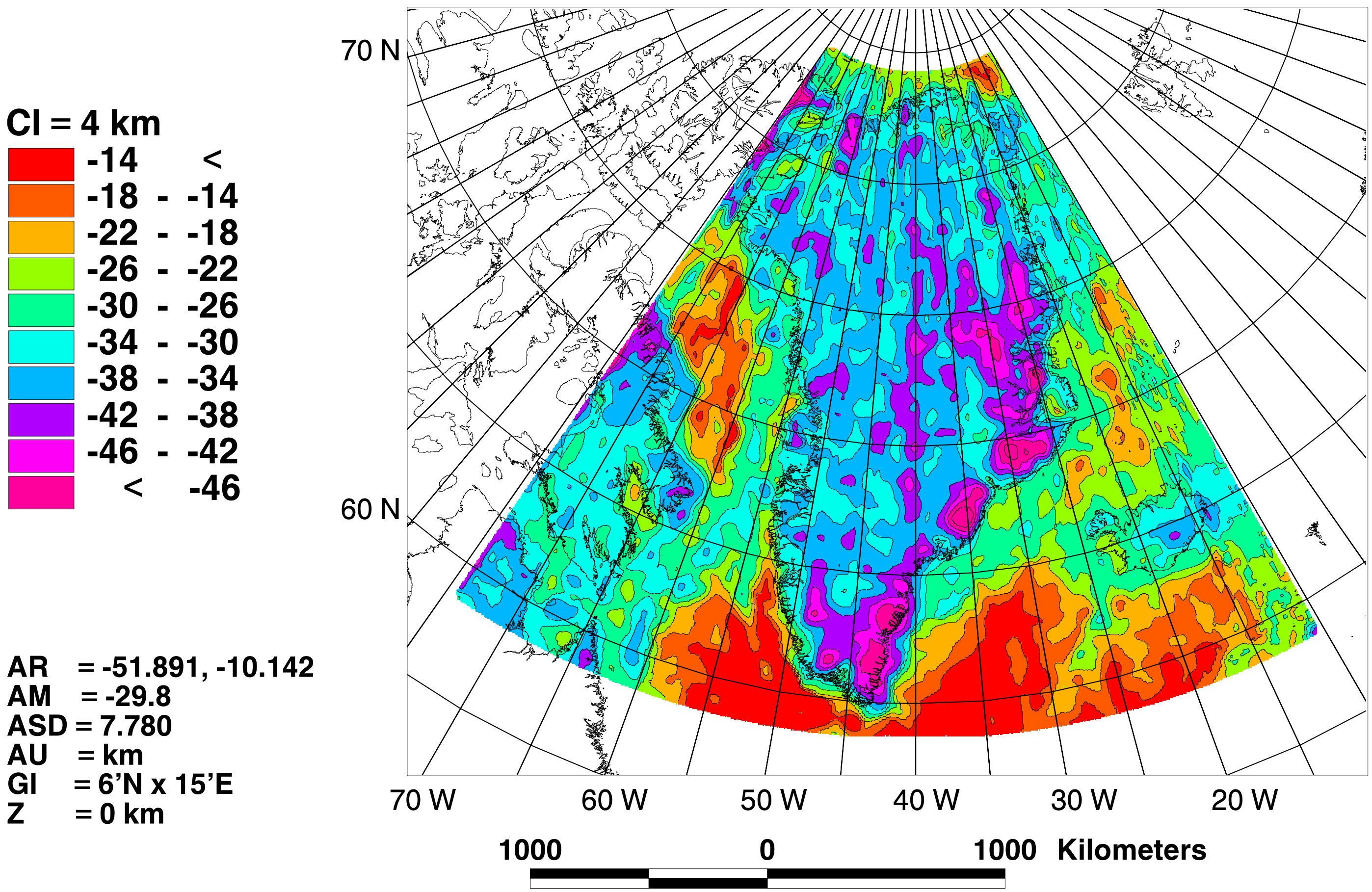

Figure 4.1: Gravity-derived Moho model for the Greenland area in a Lambert Equal-Area Azimuthal Projection centered on 40° W.

the age of crust, cratonic origin, and rock types of the midcontinent and Greenland crusts.

4.2.1 Geologic Provinces

As shown in Figure 4.2.1, southern Greenland is composed of the Ketilidian mobile belt, South Greenland Archean complex, and Nagssugtoqidian mobile belt. The Ketilidian mobile belt represents an early Proterozoic (1850-1830 Ma) orogen composed of felsic granites, reworked gneisses and migmatized older metasediments and metavolcanics [Escher and Watt, 1976]. A border zone to the north is composed of sedimentary rocks, felsic volcanics, and underlying Archean gneisses [Brozena, 1995]. Immediately to the north of this border zone is the South Greenland Archean complex (3750-2500 Ma) of quartzo-feldspathic gneisses with younger granitic and basic intrusions. The Nagssugtoqidian mobile belt (2700-1700 Ma) north of the craton is composed of strongly deformed gneisses aligned in linear sheared belts that grade into granites, granodiorites, diorites, and gabbros to the north. Some regions within this belt are composed of domes of undeformed Archean rocks.

Central Greenland is dominated by the Rinkian fold belt (1870-1650 Ma). This belt formed after cratogenic conditions were established and permitted the accumulation supracrustal sedimentary rocks and felsic intrusives. Brozena [1995] identified an additional zone of a possible magmatic arc related to Tertiary hotspot activity to the north of the Nagssugtoqidian mobile belt. He also identified an East Greenland Archean complex of gneisses to the east of the magmatic arc and southwest along the coast from the Blosseville Kyst. Tertiary volcanics on Diskó Island and the Blosseville Kyst region of Scoresby Sund are composed of picritic basalts and sedimentary rocks.

Northern Greenland is composed of the North Greenland Archean complex, a platform region where Proterozoic and Lower Paleozoic sedimentary rocks overlie the

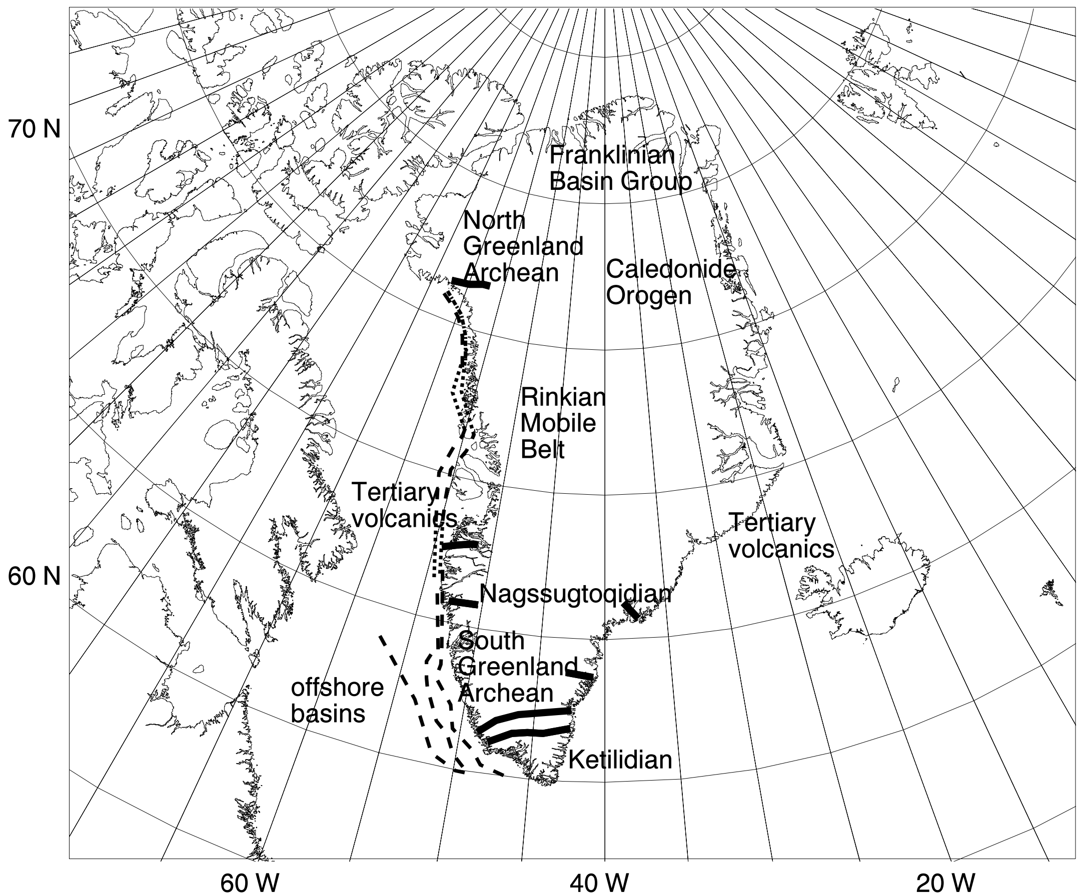

Figure 4.2: Geographic map detailing Greenland geologic provinces and the locations for the crustal structure in the southwestern Greenland margin determined in Chapter 3. Mapped boundaries in the coastal regions of Greenland were adapted from Escher and Pulvertaft [1995].

crystalline basement rocks and the North Greenland fold belt. The North Greenland Archean complex is exposed in limited outcrops [Escher and Pulvertaft, 1995] in the north and west that include mostly gneisses and more limited exposures of schists, anorthosites, amphibolite, marble, granites, and gabbros [Escher and Watt, 1976]. This platform province is overlain primarily by sedimentary rocks of the Franklinian Basin Group. The Independence Fjord Group is located between the sedimentary and the basement rocks in the interior northeast. Ineson and Peel [1997] and Dawes [1997] both provide insight into the major stratigraphic units that compose the sedimentary rocks within these regions. The North Greenland fold belt is a continuation of the Innuitian orogenic system of Arctic Canada and is composed mainly of the Franklinian Basin Group that was thrust over rhyolitic volcanics.

The Caledonian Orogen extends along the northeast and east coast and consists of extensive Archean and Proterozoic gneisses and younger geosynclinal sedimentary rocks, which are all folded, metamorphosed and later cut by granites. This orogenic belt extends onto the northeast corner of Ellesmere Island.

Offshore, most regions around the Tertiary volcanics are characterized by the build up of a basaltic volcanic platform [Escher and Pulvertaft, 1995]. Some localities off the east coast are characterized by thickened sedimentary sequences (> 4 km), some of which are cut by Tertiary dikes. On the southwest coast, deep (3 km) uninvestigated basins exist parallel to shore, and these grade into shallower regions to the north in the Davis Strait area. Broad regions of transitional crust up to 150 km wide are noted for the west coast, while transitional crust for the east coast is confined to much narrower regions (20 km).

4.2.2 Greenland Rock Densities and Magnetizations

Table 4.1 gives the range of volume magnetic susceptibilities and density variations for the various rock types of the Greenland area [Escher and Pulvertaft, 1995; Okulitch, 1991]. Table 4.1 is taken in part from Jones [1988] who studied the Precambrian basement rocks of Ohio, which exhibit similar lithologies to those found in the Greenland area. Additional density and magnetization data are also summarized in Table 4.1 from other studies [Turcotte and Schubert, 1982; Ahrens, 1995; Toft and Arkani-Hamed, 1993].

Table 4.1 provides only a broad generalization of the physical property variations for the igneous and metamorphic rocks of the study region. Sedimentary rocks for the purposes of this study were basically taken to be non-magnetic with relatively low densities in the range 2.6 - 2.7 gm/cm^3. Entries in Table 4.1 containing "NA" indicate that no data were available.

The rocks listed in Table 4.1 are grouped in Table 4.2 according to their density and susceptibility contrasts relative to gneisses. Gneisses were selected as the standard country rocks because they formed the older Archean platform and can be found in many of the younger provinces in deformed or undeformed states.

Hence, lithologies characterized by densities lower than gneisses are listed in the left column of Table 4.2, while densities higher than gneisses are in the right column. Rocks having about the same density are in the same column. Similarly, lithologies having lower magnetizations than gneisses are in the top row, and those with higher magnetizations are in the bottom row, while those with equivalent magnetizations are in the same row. The middle entry of Table 4.2 lists rocks that may also exhibit no contrast in physical properties with the gneisses.

The groupings in Table 4.2 are useful for considering the interpretation of correlative FAGA and MA. However, considerable care must be exercised in using Table 4.2

Rock Type	Density Range (gm/cm^3)	Density Average (gm/cm^3)	susceptibility Range (nT)	susceptibility Average (nT)
IGNEOUS				
Basalt	2.70-3.30	2.99	200-145,000	60,000
Granite	2.31-2.99	2.64	0-40,000	2,000
Granodiorite	2.67-2.79	2.73	NA	NA
Diorite	2.72-2.99	2.86	500-100,000	70,000
Gabbro	2.70-3.50	3.03	800-72,000	60,000
Anorthosite	2.64-2.92	2.78	NA	NA
Average	2.09-3.17	2.69	2700-270,000	NA
acidic (felsic)	2.30-3.11	2.61	38-82,000	NA
basic (mafic)	2.09-3.17	2.79	550-120,000	NA
METAMORPHIC				
Schist	2.39-2.90	2.64	300-2,400	1,200
Marble	2.60-2.90	2.70	NA	NA
Metasediments	NA	NA	200-2,000	NA
Gneiss	2.56-3.15	2.70	100-20,000	NA
Amphibolite	2.79-3.14	2.96	NA	600
Serpentine	NA	2.78	3,100-18,000	NA
Average	2.40-3.10	2.74	NA	NA

Table 4.1: Summary of Greenland area crustal rock types and associated density and volume magnetic susceptibility variations.

because there are many exceptions to these associations and the effects of magnetic remanence, which are poorly known for the rocks of Greenland, have been ignored.

4.3 Methodology for Estimating Crustal FAGA and MA and Their Correlations

The Earth's free-air gravity anomaly (FAGA) and magnetic anomaly (MA) fields result from the cumulative effects of lateral density and magnetization contrasts due to compositional, structural, and thermal variations in the crust, mantle and core. By modeling some of these components, insight on the remaining components may

Relative MA Magnitudes	Relative FAGA Magnitudes: Minima (-)	Intermediate	Maxima (+)
Minima (-)	Sedimentary Rocks Anorthosite Zones of Granitization Granite	Marble	Unaltered Ultramafics
Intermediate	Granite (magnetite rich) Felsic Extrusive Granodiorite	Gneiss Schist	Amphibolites Metavolcanics Granulites
Maxima (+)	Intermediate Extrusive Serpentine	Diorite Mafic Extrusive Serpentine	Ultramafic Intrusions Mafic Intrusions

Table 4.2: Chart of generalized correlative crustal lithologies for Greenland. Anomaly magnitudes are relative to source physical property contrasts with gneisses.

be obtained. This new insight may be used subsequently to help refine models for the evolution of the Earth's structure, composition, and processes.

By modeling the gravity effects of the components of the crustal surface (e.g., sea water, bedrock, and ice), strong positively or negatively correlative features in FAGA may be determined by spectral correlation analysis [von Frese et al., 1997]. If this terrain is accommodated by thickness variations of the crust as is suggested by an Airy-Heiskanen model of isostatic equilibrium, then the terrain-correlated FAGA may reflect regions that are over- or under-compensated. Additionally, regions undergoing dynamic uplift (e.g., above a thermal plume) also would produce a correlative signal between the FAGA and the gravity effects of the terrain. Taken together, these signals represent the terrain-correlated components (TCFAGA) of FAGA. The remaining terrain-decorrelated components (TDFAGA) of FAGA may hence most strongly reflect compositional or structural variations in the crust, mantle or core.

Subcrustal components of FAGA may be isolated by correlating TDFAGA with higher frequency components of the EGM96 [Lemoine et al., 1997; 1998a; 1998b] spherical harmonic model, which presumably are most representative of crustal sources. However, the higher degree components may also reflect sources in the lithosphere, whereas the residual lower degree components are more consistent with the effects of sources in the mantle or core, and thus may provide important constraints on processes in these regions, such as mantle upwelling and hotspot effects.

The parts of TDFAGA that do not correlate strongly with the higher harmonics are termed mantle-core components (MC-TDFAGA) of TDFAGA, whereas those which correlate are called the intracrustal components (IC-TDFAGA) of TDFAGA. However, IC-TDFAGA may not completely reflect crustal sources because the upper mantle material immediately beneath the crust is still sufficiently shallow to also generate higher frequency components in FAGA. Therefore, the sources that generate IC-TDFAGA may not solely arise in the crust but also from the upper mantle, which together comprise the lithosphere. To further separate the crustal and mantle components in IC-TDFAGA, comparison with MA may be made.

For the Greenland study area, the magnetic properties of the crust tend to increase with depth to the Moho or the Curie isotherm of magnetite if it it shallower [Shive et al., 1992]. For purposes of this study, the Moho is taken as the magnetic boundary, so that the sources of MA are assumed to be limited to the crust.

The component of the MA due to crustal thickness variations may be estimated and removed by using the crustal thickness model for this region developed in Chapter 3. The gravitational effect of this crustal mass was modeled by Gaussian Legendre quadrature integration assuming densities of 2.8 gm/cm^3 for continental crust and 2.9 gm/cm^3 for oceanic crust. Regions of oceanic crust were generally defined as being located in water deeper than 1 km [Kerr, 1980]. The radial derivative of the gravity model may then be used to generate pseudo-magnetic anomalies (PMA) that can be related to the radial (r) component of MA (RTPMA) by Poisson's Relation [e.g., Blakely, 1995], which is given by:

$$MA(r) = -C\frac{m}{G\rho}\frac{\partial \Delta g}{\partial r} \tag{4.1}$$

where: $RTPMA = MA(r) =$ radial (r) component of magnetic anomalies
$C =$ proportionality constant
$m =$ susceptibility
$G =$ gravitational constant
$\rho =$ density
$\Delta g =$ free-air gravity anomalies
$r =$ radial direction

By spectral correlation analysis of the RTPMA and PMA, the component of the RTPMA most positively correlated to PMA may be extracted as the magnetic anomalies related to variations in crustal thickness. The residual terrain-decorrelated components (IC-RTPMA) of MA hence may reflect lateral variations of the magnetization within the crust.

The IC-TDFAGA and IC-RTPMA may be combined for favorability indices that help establish the distribution of correlative features [von Frese et al., 1997]. In particular, the data sets may be normalized so that they produce unbiased sums, differences, and quotients that highlight positively, negatively, and null correlated features, respectively. Summing the normalized data sets yields summed local favorability indices (SLFI) that map out positively correlative features (e.g., correlative maxima or minima in IC-TDFAGA and IC-RTPMA). Differencing the normalized data sets yields differenced local favorability indices (DLFI) that highlight negatively correlated features (e.g., IC-TDFAGA maxima with IC-RTPMA minima and vice versa). Quotients of the normalized grids (QLFI), where the absolute value of the denominator grid is used, will yield large positive and negative QLFI where features in the numerator grid are not matched in the denominator grid. Additionally, QLFI ~ 0 where features in the denominator grid are not matched in the numerator grid, and QLFI $\sim \pm 1$ where features in the two grids are correlative.

The SLFI, DLFI and QLF will be examined, and the densities and magnetic susceptibilities that these anomalies suggest will be related to the poorly understood geologic features of Greenland that are presented in Figure 4.2.

4.4 Terrain-Decorrelated Free Air Gravity Anomalies

Free-air gravity anomalies (FAGA) from the National Imagery and Mapping Agency were processed in Chapter 3 to determine components that were correlative and non-correlative with the gravity effects of a terrain model for the Greenland region (58.7 - 84.2°N and 285.75 - 349.50°E).

With the removal of the terrain-correlated components from FAGA, the remaining terrain-decorrelated components (TDFAGA) may reflect lateral and vertical density variations within the crust and from deeper sources and are shown in Figure 4.3. These TDFAGA are now further refined to better isolate the lateral density variations within the crust by removing those TDFAGA components related to deeper sources. Possible identification of these components may be facilitated by comparing TDFAGA with FAGA predictions determined from the EGM96 spherical harmonic coefficients [Lemoine et al., 1997; 1998a; 1998b].

4.4.1 Correlation Analysis with EGM96

The TDFAGA reflect crustal and subcrustal components that may be separated using the EGM96 gravity field spherical harmonic coefficients [Lemoine et al., 1997; 1998a; 1998b]. This 360 degree model was derived from a global data base and has a minimum wavelength of 111 km. The lower harmonics ($<$ 100 degree) are more often associated with subcrustal mass variations within the Earth, such as mantle plumes and phase changes [Anderson, 1998]. Higher harmonics reflect the shallower features that cannot be observed at depth due to attenuation (e.g., a 111

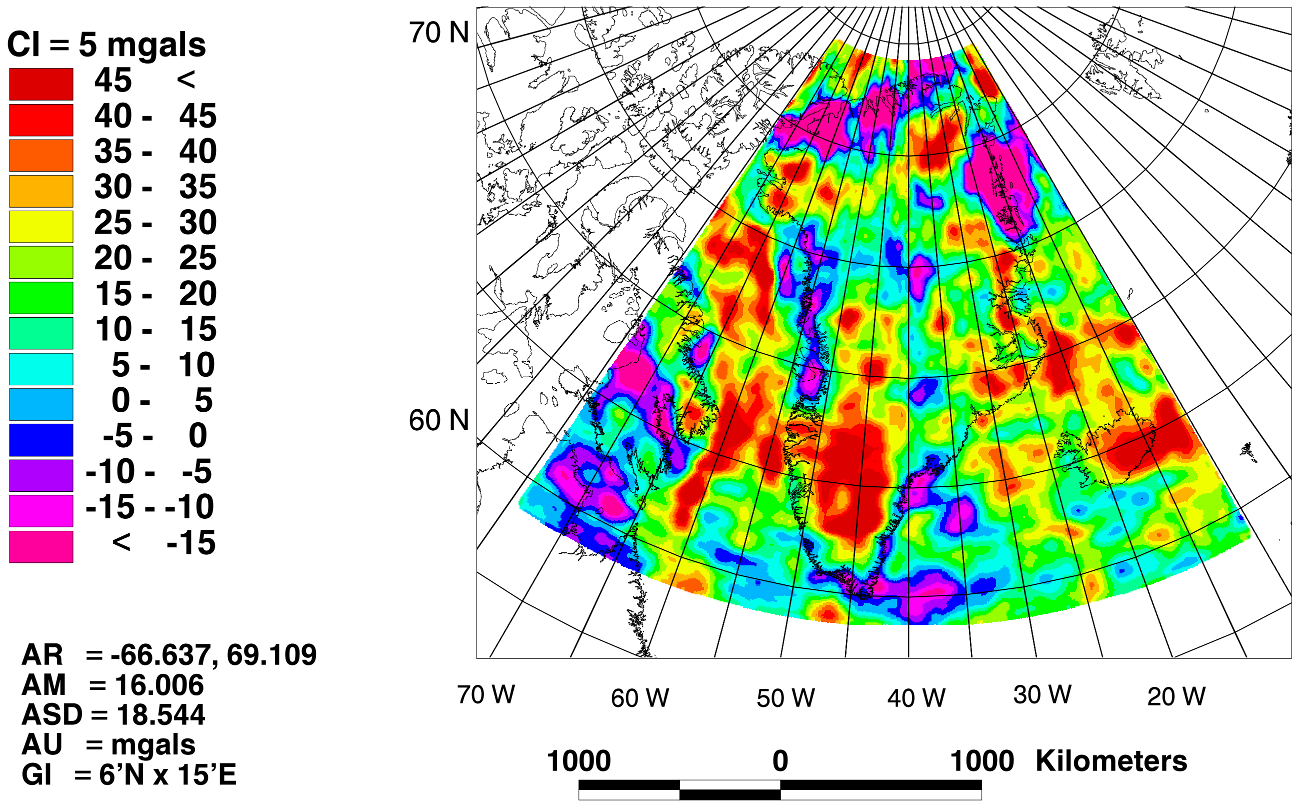

Figure 4.3: Terrain decorrelated FAGA (TDFAGA) in a Lambert Equal-Area Azimuthal Projection centered on 40°W at 20 km above MSL. These data represent that component of the reference FAGA that is left over after removal of TCFAGA.

km feature located at the core-mantle boundary would not be resolved in the gravity field measured at the Earth's surface). Therefore, shallower features dominate the higher harmonics, whereas the lower to intermediate harmonics may reflect either shallow or deep features.

To separate out the TDFAGA components more related to shallower features, FAGA derived from the EGM96 coefficients were used. The correlation between the TDFAGA and cumulative EGM96-FAGA generated from degree 360 to degree 5 at five degree intervals was investigated. This was accomplished by generating the full 360 degree EGM96-FAGA field and removing the degree 355 field. Differences between these models arise from degrees 356 through 360. This process was repeated to generate fields at degrees 350 to 5 at 5 degree intervals. Figure 4.4.a shows the percent coherencies between TDFAGA and EGM96-FAGA calculated cumulatively from high to low degrees (solid line) and low to high degrees (dashed), whereas Figure 4.4.b gives the horizontal derivative of the solid line. The two profiles in Figure 4.4.a cross at degree 62, while the slope break in Figure 4.4.b is clearly seen at degree 100.

At degree 62, TDFAGA correlates equally with the EGM96-FAGA derived cumulatively from the lower harmonics (below degree 62) and the higher harmonics (above 62). However, the significance of the cross-over is not clear at present for isolating crustal sources. EGM96-FAGA from harmonics lower than degree 100 generated most of the coherent signal with the TDFAGA. Sources for these features could be either deep or shallow regional features. Features more related to harmonics higher than degree 100 are more likely to derive from shallow (crustal or upper mantle) sources only, because of attenuation of the gravity signal for shorter wavelength features. As only the components of TDFAGA related to crustal sources (IC-TDFAGA) are desired, only the EGM96-FAGA derived from coefficients higher than degree 100 are of interest and these are shown in Figure 4.5.

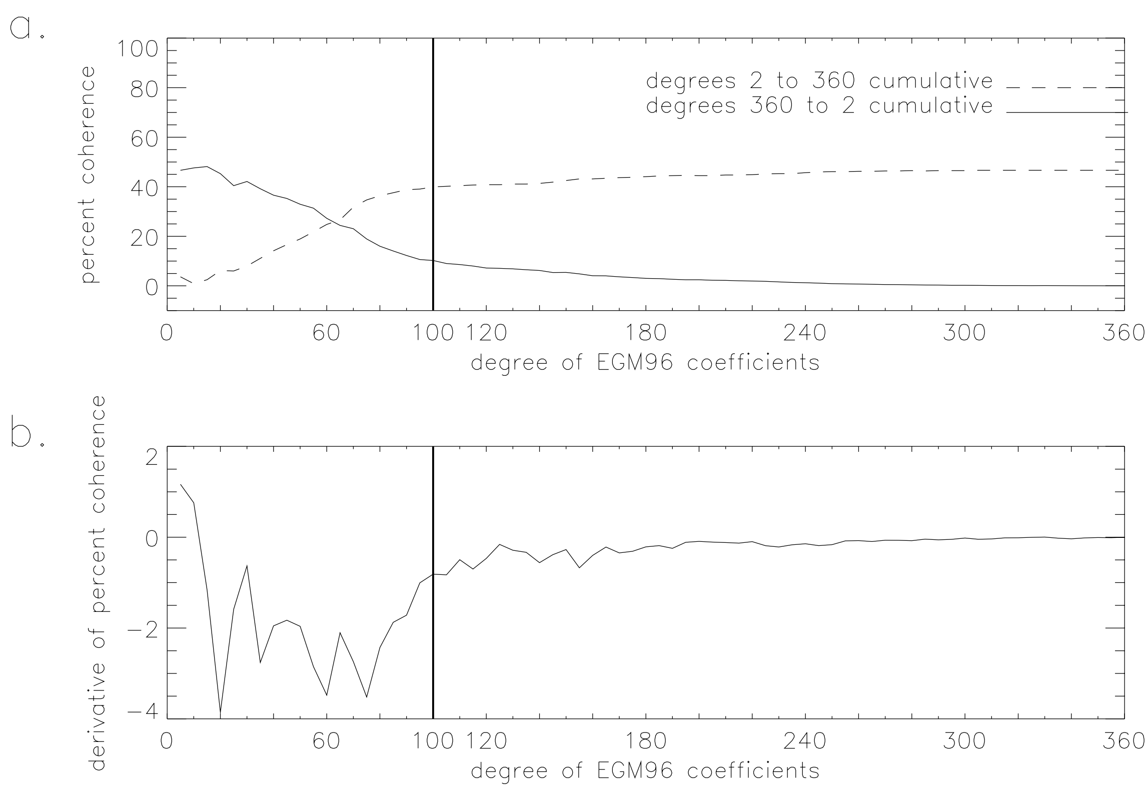

Figure 4.4: Percent coherence versus cumulative harmonics. **a.** The terrain decorrelated portion of NIMA's FAGA (TDFAGA) were correlated with FAGA generated by the cumulative EGM96 harmonics from degree 360 to 2 (solid) and from degree 2 to 360 (dashed). Note the slope break at degree 100. Harmonics lower than 100 generate most of the agreement between the data sets. The effects modeled by harmonics over degree 100 are assumed to be representative of shallower sources in the lithosphere, having shorter wavelengths and less power. **b.** First horizontal derivative of the profile for degrees 360 to 2. The thickened vertical line highlights the slope break at degree 100.

These anomalies tend mostly to highlight coastal and intraplate features such as the coast parallel ridges in the southwest, the Tertiary volcanic provinces of Diskó Island and Blosseville Kyst, as well as numerous smaller features within central-northern Greenland. Hence, degrees 101 through 360 components appear to show a relatively strong affinity with features of the crust or shallow mantle (i.e., the lithosphere).

The asthenosphere underlies the lithosphere and represents a region that is less viscous and less apt to retain short wavelength features. Deeper is the mesosphere that starts at about 400 km depth, which is characterized by relatively rigid behavior and large density contrasts created by phase transitions at about 400 and 700 km [Press and Siever, 1982]. Anderson [1998] has weakly linked these mantle phase transitions with 400 to 1000 km features of the Earth's gravity field that are equivalent to degrees 100 to 9, respectively, in a spherical harmonic model. Hence, the EGM96 gravity field will be divided into components derived from harmonics below and above degree 100 for further analysis.

The EGM96-FAGA components with degrees lower than 100 shown in Figure 4.6 are characterized by prominent gravity anomalies near the Reykjanes Ridge (RR) spreading center, Nares Strait (NS) plate boundary, Caledonian Orogen (CO), Davis Strait (DS) plate boundary, and deep roots under eastern and southern Greenland. The regional features in Figure 4.6 may reflect deeper and larger scale features in the crust or mantle (e.g., variations of the core-mantle boundary) and have more power than EGM96-FAGA components derived from harmonics higher than 100 in Figure 4.5 where smaller portions of the total gravity signal are generated [Anderson, 1998].

The components of TDFAGA that were most correlative with the EGM96-FAGA derived from degrees 101 to 360 are more likely related to intracrustal or crust/mantle

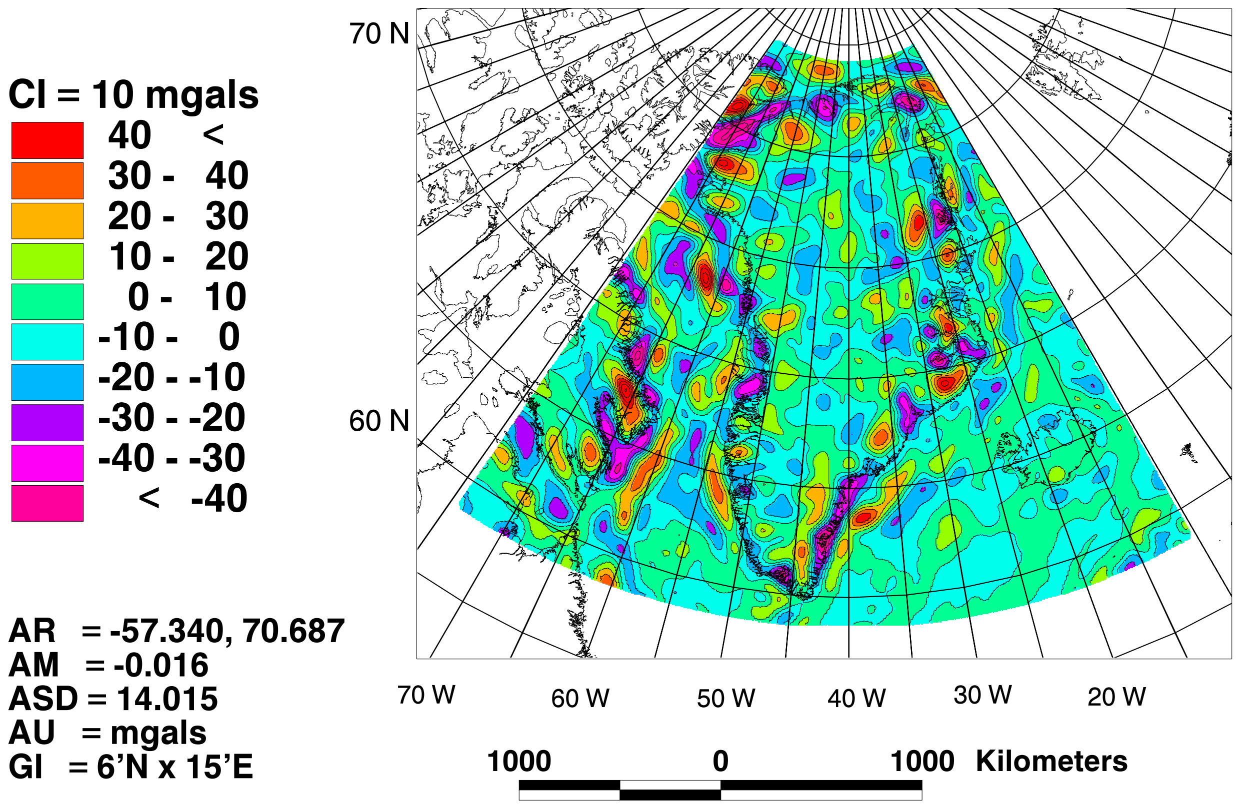

Figure 4.5: EGM96-FAGA derived from degrees 101 to 360 EGM96 coefficients in a Lambert Equal-Area Azimuthal Projection centered on 40° W.

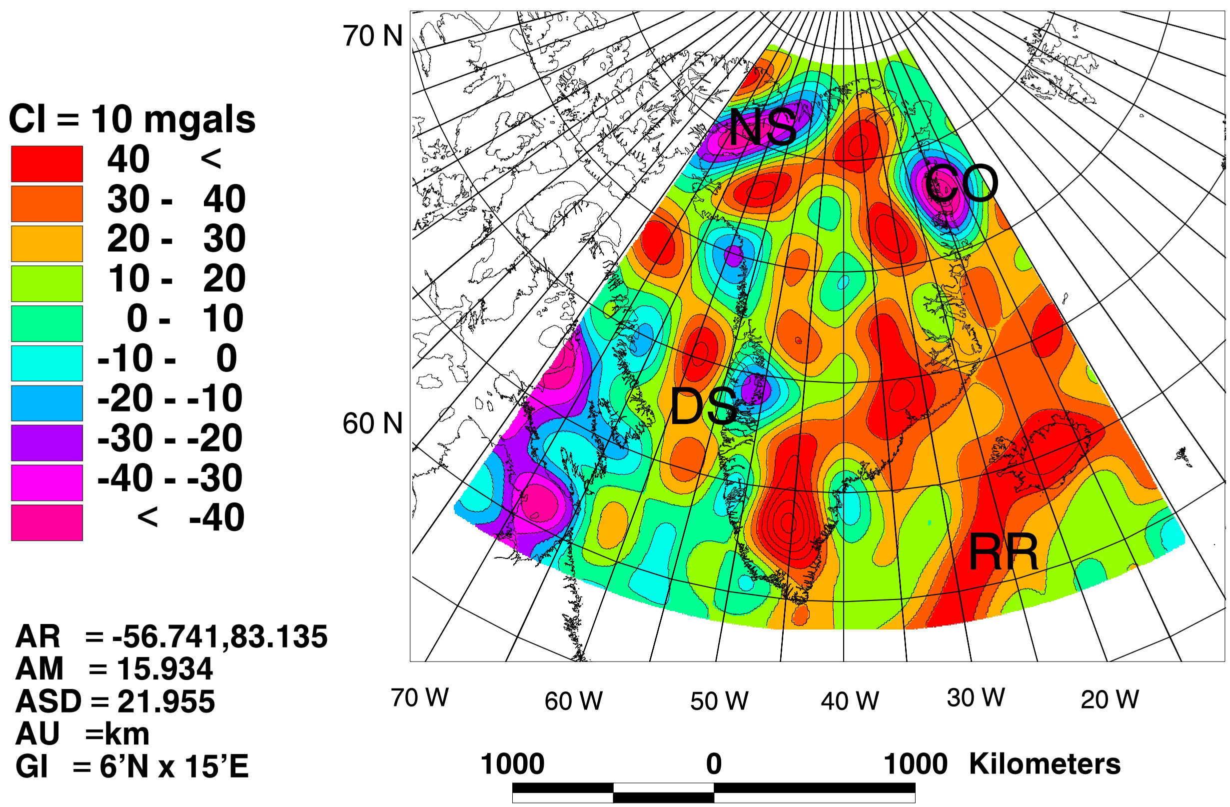

Figure 4.6: EGM96-FAGA data derived from degrees 2 to 100 EGM96 coefficients in a Lambert Equal-Area Azimuthal Projection centered on 40° W. Labels refer to geologic features discussed in the text.

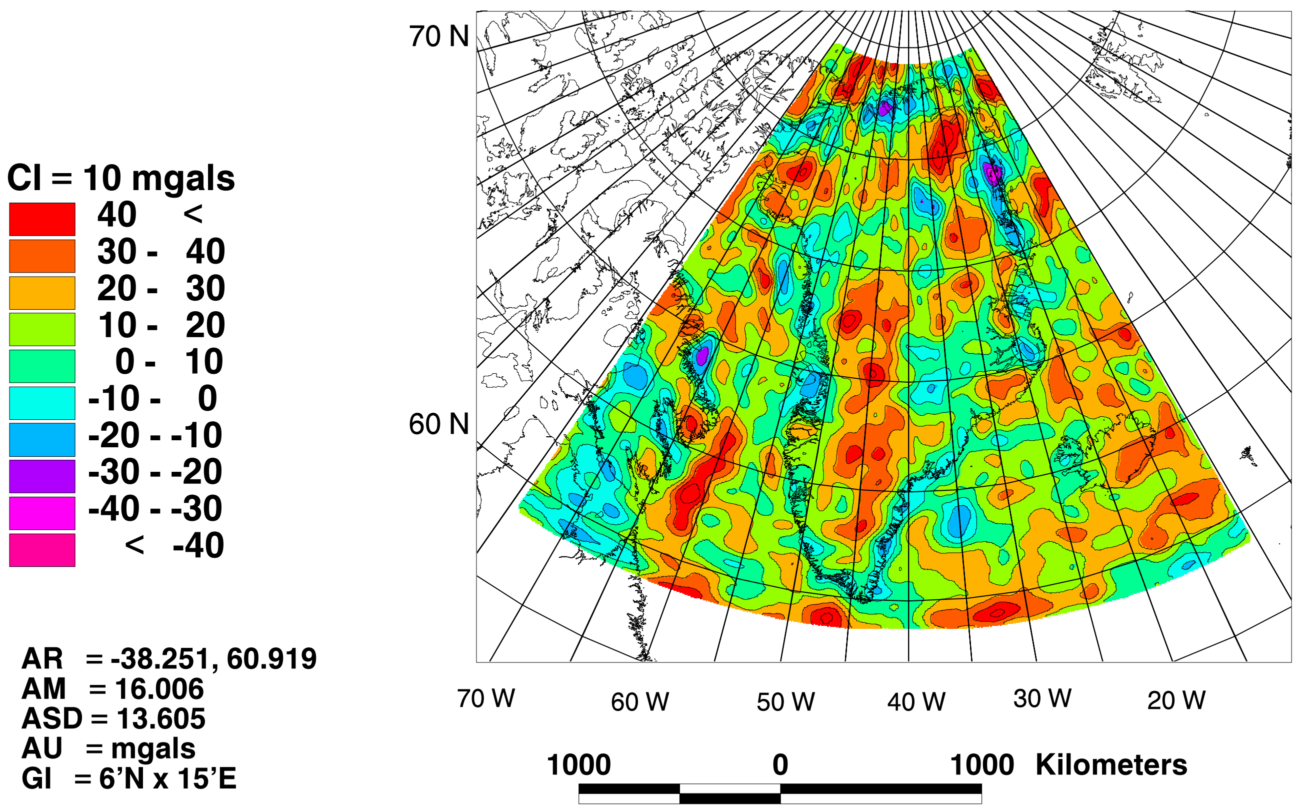

Figure 4.7: Intracrustal components of the terrain-decorrelated gravity anomalies (IC-TDFAGA) in a Lambert Equal-Area Azimuthal Projection centered on 40° W. These data represent that portion of TDFAGA that may be more related to lithospheric sources as determined by their coherency with EGM96-FAGA data derived from degrees 101-360 (Figure 4.5).

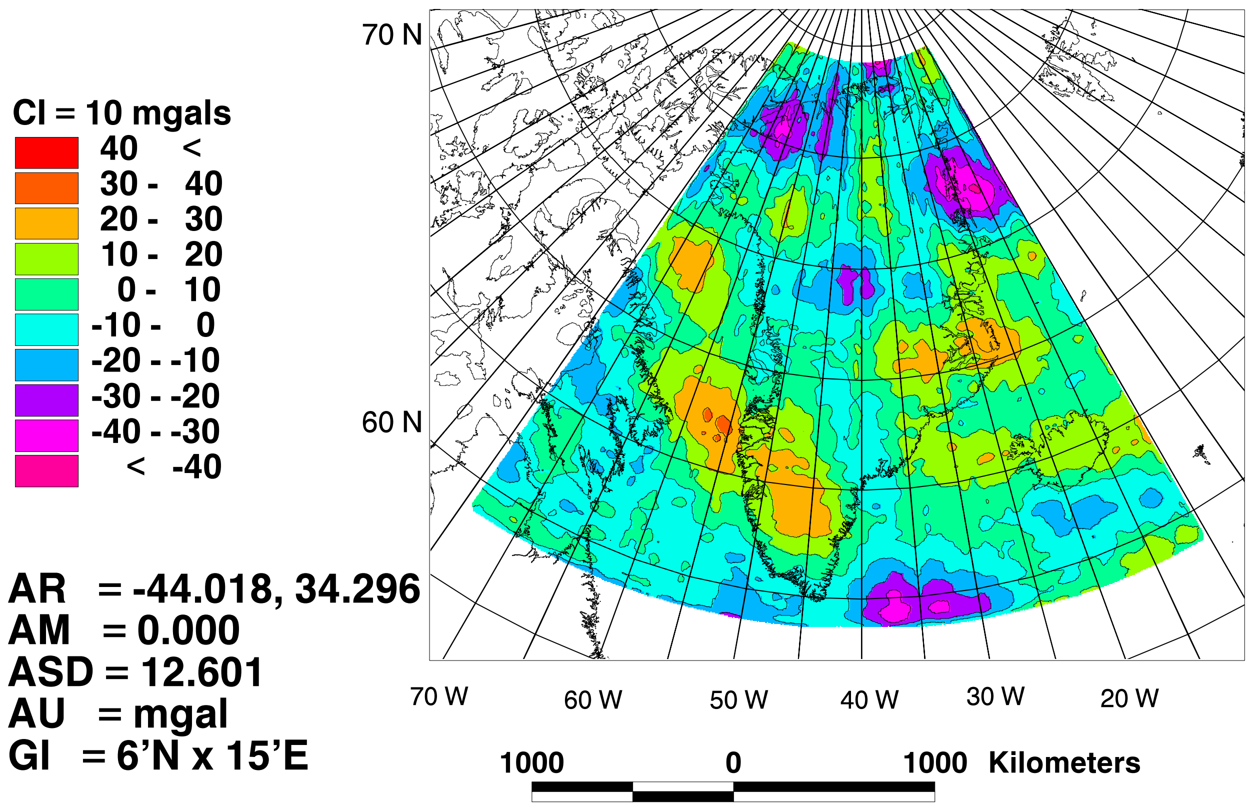

Figure 4.8: Residual TDFAGA (TDFAGA - IC-TDFAGA) in a Lambert Equal-Area Azimuthal Projection centered on 40° W. These data may be more related to the lower harmonics (2 to 100) of EGM96 but also contain high frequency signal that may be noise-related.

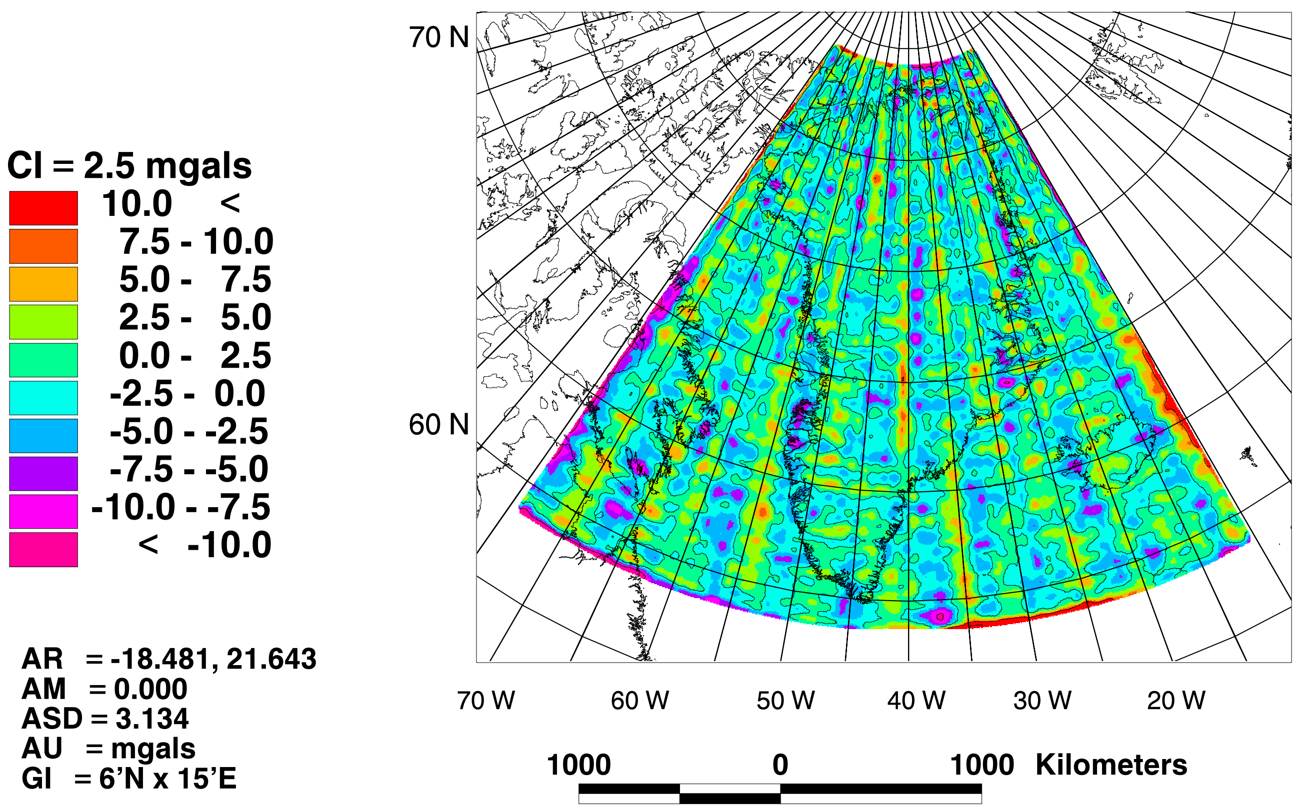

Figure 4.9: Residual TDFAGA high-pass filtered at 400 km in a Lambert Equal-Area Azimuthal Projection centered on 40° W. These data have little power and are oriented along the grid intervals suggesting that they may be more related to grid processing.

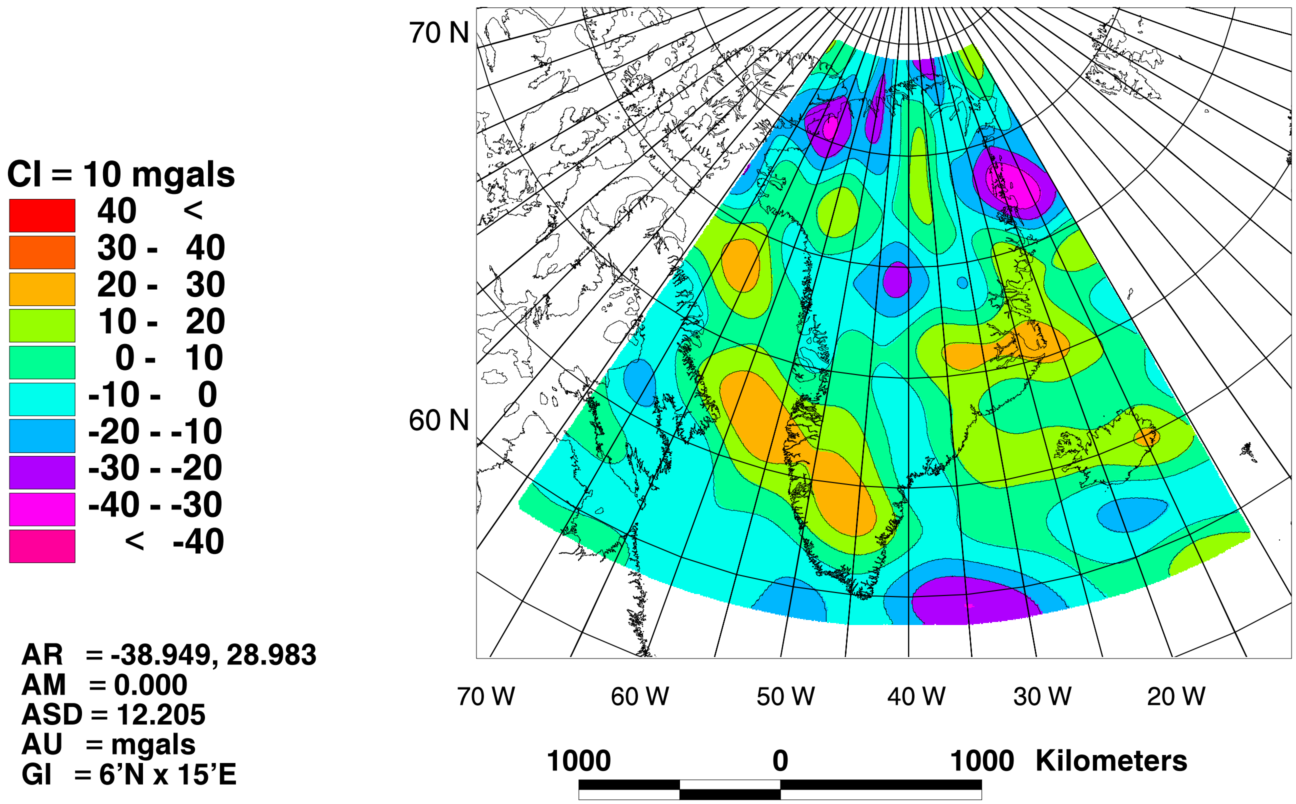

Figure 4.10: Residual TDFAGA low-pass filtered at 400 km (MC-TDFAGA) in a Lambert Equal-Area Azimuthal Projection centered on 40° W. These data represent the long wavelength component of the NIMA-derived FAGA that are least correlated with surfacial features and most correlated with deeper sources.

boundary features (IC-TDFAGA) and are shown in Figure 4.7. The IC-TDFAGA will be used in the comparison with the MA, but the residual TDFAGA warrant further examination also.

Residual TDFAGA shown in Figure 4.8 were generated by removing IC-TDFAGA from TDFAGA. The residual TDFAGA contained both long and short wavelength data but should be composed primarily of longer wavelengths related to degrees 2 to 100 of the EGM model. Since degree 100 corresponds to about a 400 km wavelength, these data were filtered at 400 km to separate the short and long wavelength aspects. The shorter wavelengths of the residual TDFAGA are shown in Figure 4.9 and demonstrate nodal organization that corresponds to the grid interval. These data have very little power (ASD=3 mgals) compared to the original data (ASD=13 mgals) and probably represent systematic errors related to gridding and processing. The longer wavelengths of the residual TDFAGA shown in Figure 4.10 are much smoother and regional in nature, and may reflect mantle or core sources in TDFAGA (MC-TDFAGA) associated with mantle plumes and hotspots. These data will be considered further after processing the MA for comparison with the IC-TDFAGA.

4.5 Terrain Decorrelated Magnetic Anomalies

Shive et al. [1992] shows that for the Greenland study area and surrounding regions, the thickness of the magnetic crust may be on the order of the depth to Moho (i.e., magnetic sources may be confined essentially between the surface and the Moho). Hence, removal of the MA components that vary according to crustal thickness will leave that portion derived from lateral variations in structure and composition within the crust.

4.5.1 Data Description

The Geological Survey of Canada (GSC) compiled various airborne and shipborne surveys, as well as previously gridded MA data sets, into an Arctic MA data set [Verhoef et al., 1996]. Due to secular variation errors, leveling errors, and other uncertainties, the long wavelength components of the compilation were significantly corrupted. Hence, the components of the compilation with wavelengths greater than 400 km were removed by averaging all data inside a circle with a radius of 400 km using a Hanning function as the weight function [Verhoef et al., 1996]. This low-cut filtering also facilitated merging the data from the Greenland Aerogeophysical Projects of 1991 and 1992 (GAP '91 and '92) [Brozena, 1995] and reduced the average crossover misfit from -80.1 nT to -1.1 nT.

The resulting MA compilation has two further sources of error that were not addressed by Verhoef et al. [1996], which must be considered in any application. First, the airborne surveys were conducted at a number of different elevations with some nearly at sea level and others as a high as 4 km, such as the GAP '91 and '92 observations mapped by the Naval Research Laboratory. These data represented a critical element in assessing the MA field in Greenland, as they were used by GSC to determine the MA for interior Greenland.

Hence for this study, the MA were all upward continued to help mitigate the effects of the different survey elevations and reduce related high frequency effects at the boundaries between various data sets obtained at different elevations. The 20 km elevation was selected for the upward continuation based on the 30-km nominal track spacing of the GAP '91 and '92 data, which thus controls the spatial resolution for the MA in central Greenland. Upward continuing to elevations higher than 20 km was possible but would have degraded data in regions where the line spacing was closer than 30-km. Based on this limiting resolution, the data were regridded at an approximate 10-km interval (6'N x 15'E) and upward continued to an elevation of 20 km.

Secondly, the AGC compilation was not reduced to the pole [Roest, personal communication, 1998], so that the relationships between the MA and their subsurface sources and related gravity effects are considerably complicated by the complex properties of the Earth's Arctic core magnetic field. The MA were only defined with respect to an International Geomagnetic Reference Field (IGRF) that is updated every five years [Barton, 1996].

For this study, a reduction-to-pole (RTP) procedure was implemented to transform the MA to their equivalents (RTPMA) at the Earth's geomagnetic pole where geomagnetic inclination and declination are 90° and 0°, respectively.

To evaluate the RTPMA, a mean IGRF model was developed for 1970 through 1990 when the MA surveys had been conducted. A mean IGRF for this study area was possible because the inclination, declination and intensity values of the IGRF models over the 20 year period showed very little change at any given location. The RMS difference at all points from 1970 to 1990 was 1.1° for declination, 0.1° for inclination, and 53.6 nT for intensity.

Because of this low temporal variability, the IGRF models are averaged at 20 km elevation as shown in Figure 4.11. The spatial variability of the mean IGRF data is an order of magnitude greater than its temporal variability, where the RMS differences over the observation points in declination, inclination, and intensity are 17.3°, 4.3°, and 2097 nT, respectively.

To better account for the spatial variability of the mean IGRF, the MA were divided up into 5 blocks and reduced to the pole according to the mean declination and inclination of each block. Table 4.3 lists the mean declination and inclination for each block, each of which was 6.3° in latitude and 15.75° in longitude.

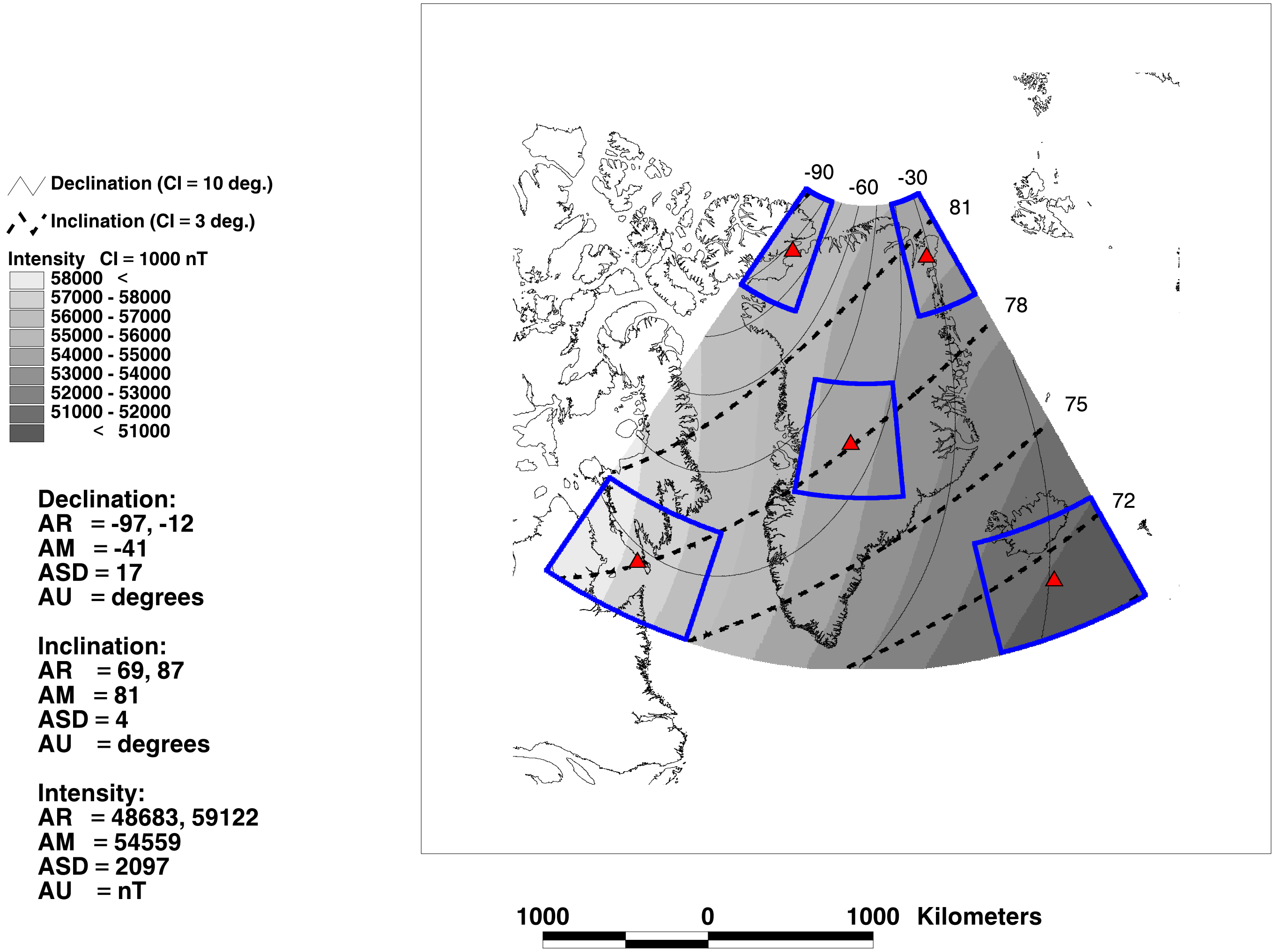

Figure 4.11: Average IGRF declination (solid line), inclination (dashed line), and intensity (grey scale) in a Lambert Equal-Area Azimuthal Projection centered on 40° W. Data were obtained and averaged from the 1 degree IGRF models for epochs 1970-1990. Blue boxes depict the five regions that were adjusted based on the inclination-declination pairs (Table 4.3) determined at the red triangle in the center of each box.

Location	Latitude (°N)	Longitude (°W)	Declination (°)	Inclination (°)
Southwest	61.800	66.500	-38.81	81.16
Northwest	81.000	66.500	-78.36	86.22
Northeast	81.000	18.500	-31.18	83.45
Southeast	61.800	18.500	-19.63	74.19
Central	71.350	42.625	-43.47	81.13

Table 4.3: Inclination and declination pairs for reduction-to-pole. Values were selected at points inset from the four corners and at the middle of Figure 4.11. The reduction-to-pole was performed for each of these pairs, and the procedure was assumed valid for approximately 700 km around each point. Values for points more than 700 km from these points represented a weighted average of the values generated by all the below pairs.

The 20 km upward continued MA data were reduced-to-pole (RTPMA) using the first 4 inclination-declination pairs given in Table 4.3. Hence, four grids were generated each based on a different inclination-declination pair. The 6.3° lat. x 15.75° lon. patch around each pair was retained, and the remaining MA outside of any block were linearly combined using inverse distance weighting to generate a merged RTPMA.

The central block was used to adjust the MA further and to test the accuracies of the merged RTPMA. RTPMA in the central block were removed from coincident merged RTPMA in the central block region. The residuals are characterized by low energy ($\sigma = 2.6$ nT), little bias ($\mu = 0.535$ nT), and small amplitudes (max/min=9.6/-14.0 nT). These residuals are clearly well within the observation errors of the MA, which have been reported to range from 25 to 100 nT [Verhoef et al., 1996].

The RTPMA for the fifth block were incorporated with the results for the other 4 blocks to generate the final RTPMA grid shown in Figure 4.12. This grid reflects the RTPMA obtained differentially for the five pairs of inclinations and declinations given in Table 4.3. Although the effects of magnetic remanence can be significant

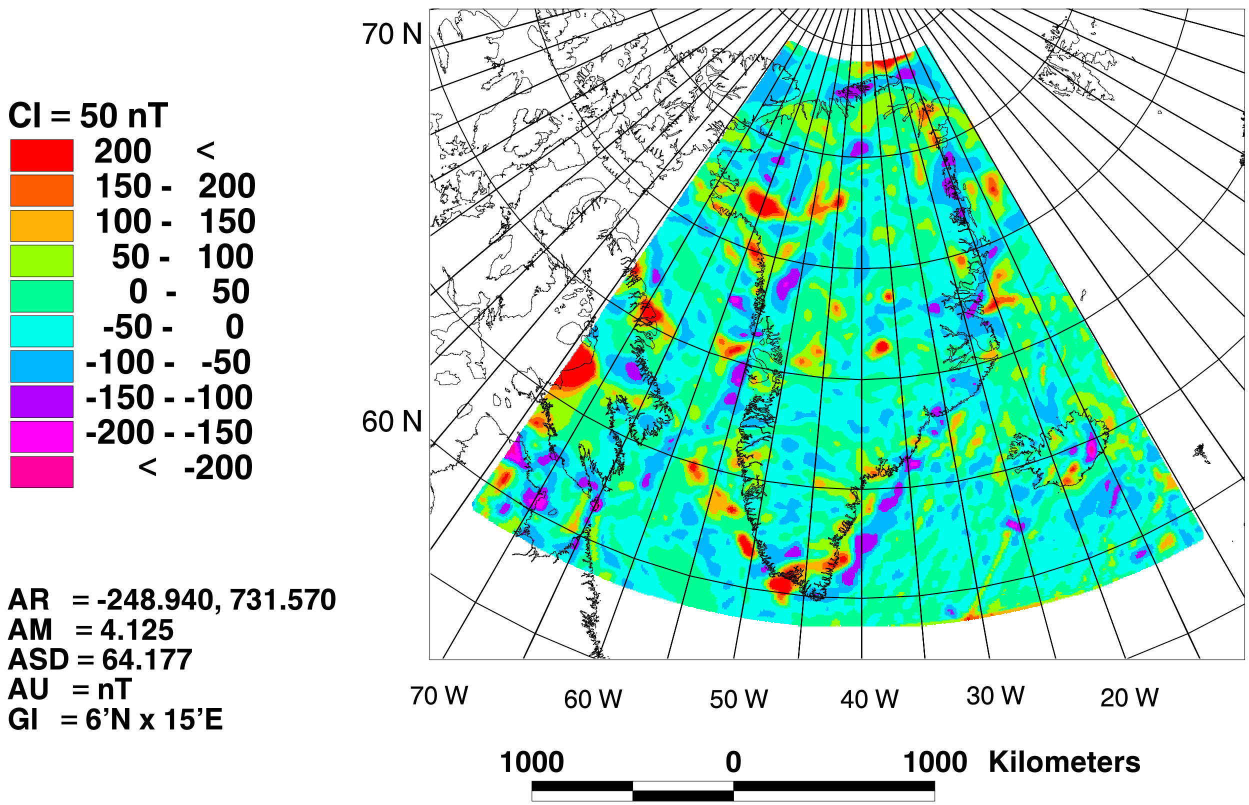

Figure 4.12: RTPMA at 20 km elevation in a Lambert Equal-Area Azimuthal Projection centered on 40° W.

[e.g., Harrison, 1987], these effects are poorly understood and have been ignored for the study region where they appear to be most prominent around the Reykjanes Ridge and the ridges of the Labrador Sea and Baffin Bay.

4.5.2 Magnetic Effects due to Crustal Thickness Variations

To a first order, magnetization increases with depth to the Moho or Curie isotherm, whichever is shallower [e.g., Wasilewski and Mayhew, 1982; 1992; Wasilewski et al., 1979]. Hence, the crustal thickness variations in Figure 4.13 may be used to estimate the related magnetic effects in the RTPMA of Figure 4.12. These effects, in turn, may be removed to estimate intracrustal magnetic anomalies (IC-RTPMA) for comparison with IC-TDFAGA.

To estimate the crustal thickness effects in Figure 4.12, the pseudo-magnetic effects represented by the first vertical derivative of the gravity effects of the thickness variations of the crust may be used. The Moho depth model shown in Figure 4.1 was subtracted from crustal DEM [Chapter 3] to determine the crustal thickness model given in Figure 4.13. GLQ integration was used to calculate the gravity effect of the crustal thicknesses assuming a density of 2.8 gm/cm^3 for continental regions and 2.9 gm/cm^3 for oceanic regions. The two regions were differentiated at the -1000 m depth on the continental slope surrounding Greenland [Kerr, 1980].

The first vertical derivative gravity effects of the crustal thicknesses (FVD(CGE)) were obtained as shown in Figure 4.15 by applying a standard vertical derivative operator to the crustal gravity data of Figure 4.14 in the frequency domain. Assuming that the thickness variations define correlative density and susceptibility contrasts, the results in Figure 4.15 may be related to the RTPMA in Figure 4.12 via Poisson's Relation in Equation 4.1. In particular, Figure 4.15 was spectrally correlated with

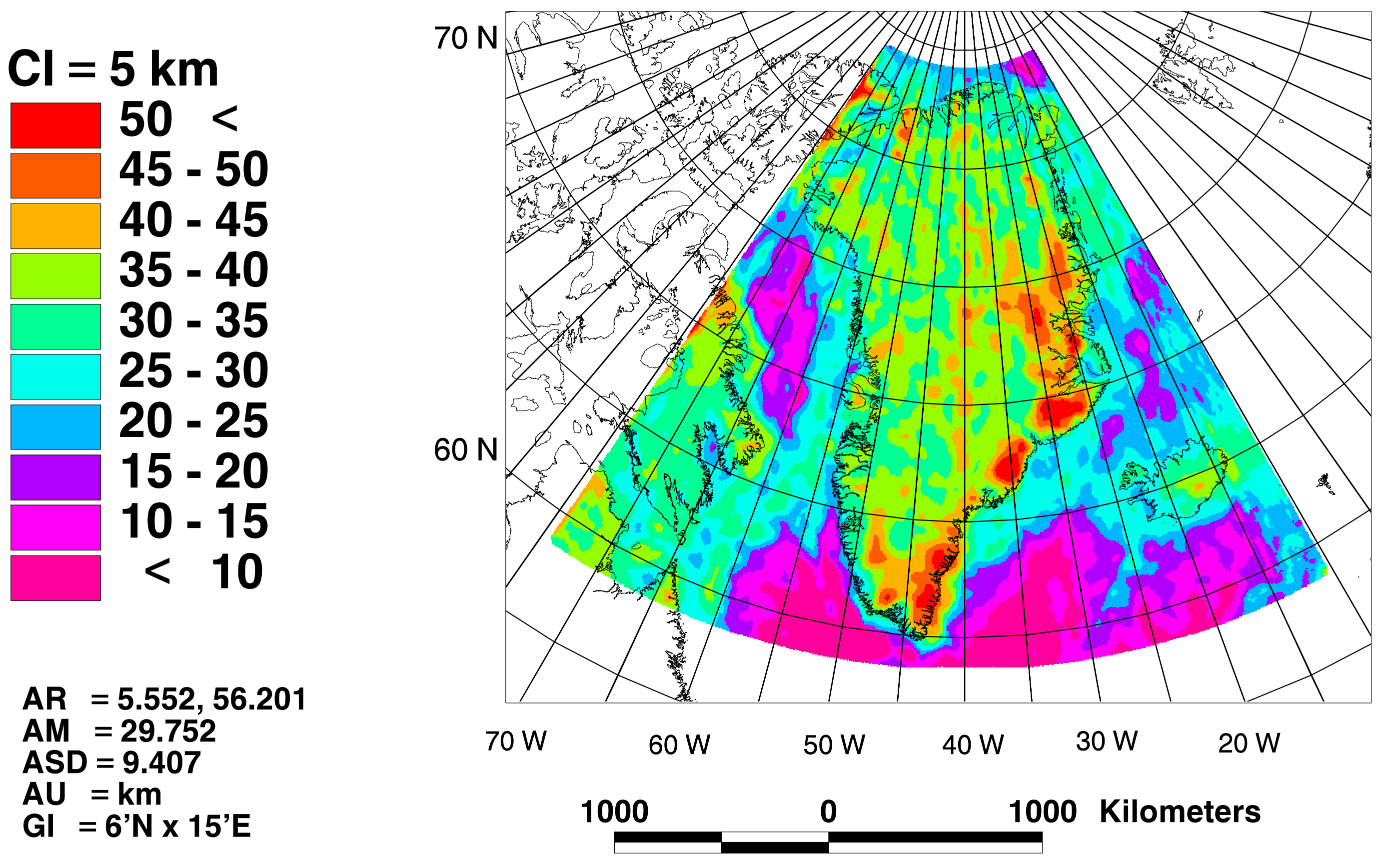

Figure 4.13: Greenland crustal thickness model derived from differencing a bedrock DEM [Chapter 3] and Moho depth model (Figure 4.1) in a Lambert Equal-Area Azimuthal Projection centered on 40° W.

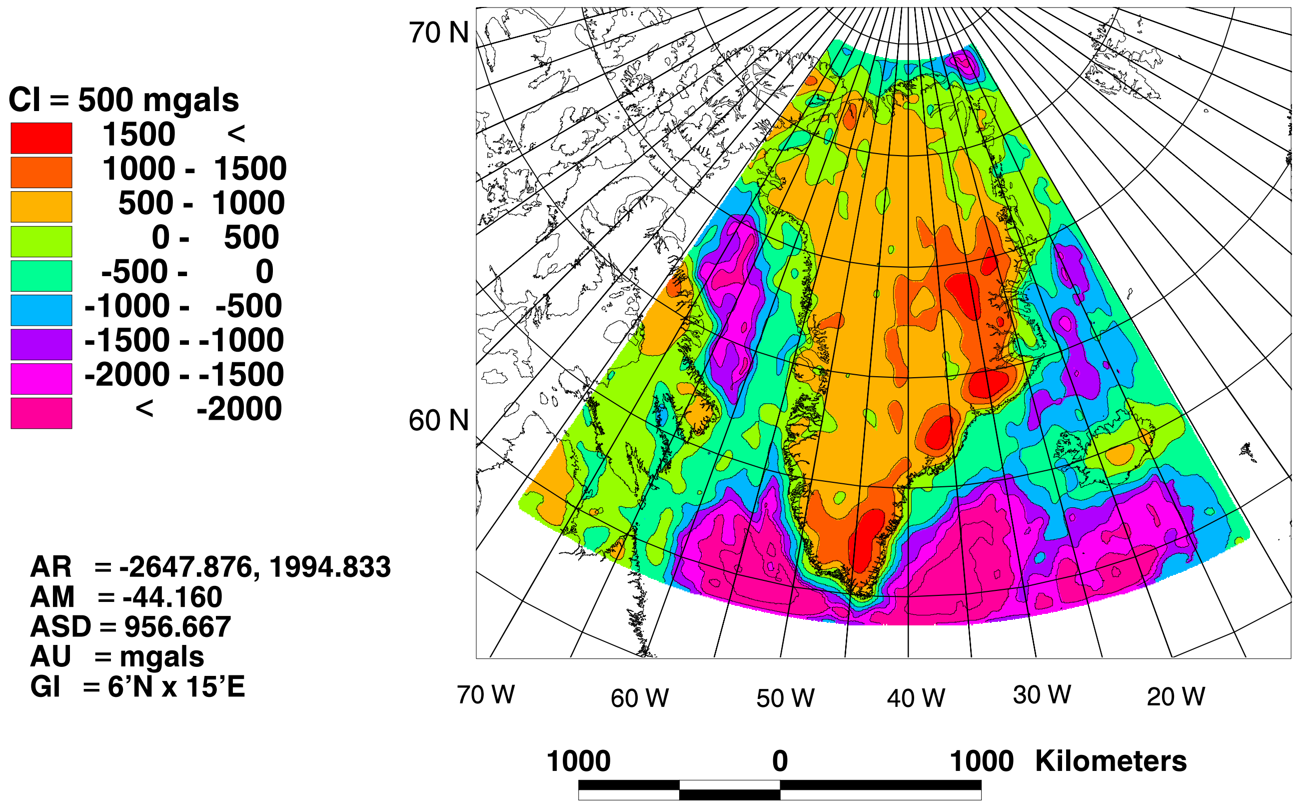

Figure 4.14: GLQ-derived gravity effect of the crustal model of Figure 3.31 in a Lambert Equal-Area Azimuthal Projection centered on 40° W.